MAGNETIC NANOPARTICLE BASED BOVINE SPERM SORTING

M.Sc. Thesis

By

SAMPURNA DASGUPTA

DEPARTMENT OF BIOSCIENCES AND BIOMEDICAL ENGINEERING

INDIAN INSTITUTE OF TECHNOLOGY INDORE

MAY 2023

MAGNETIC NANOPARTICLE BASED BOVINE SPERM SORTING

A THESIS

Submitted in partial fulfillment of the requirements for the award of the degree
of
Master of Science

by

SAMPURNA DASGUPTA

DEPARTMENT OF BIOSCIENCES AND BIOMEDICAL ENGINEERING
INDIAN INSTITUTE OF TECHNOLOGY INDORE
MAY 2023

INDIAN INSTITUTE OF TECHNOLOGY INDORE

CANDIDATE'S DECLARATION

I hereby certify that the work which is being presented in the thesis entitled "**MAGNETIC NANOPARTICLE BASED BOVINE SPERM SORTING**" in the partial fulfillment of the requirements for the award of the degree of **MASTER OF SCIENCE** and submitted in the **DEPARTMENT OF BIOSCIENCES AND BIOMEDICAL ENGINEERING, Indian Institute of Technology Indore**, is an authentic record of my own work carried out during the period from Oct 2021 to May 2023. Thesis submission under the supervision of Dr. Sharad Gupta, Associate professor,BSBE, IIT Indore.

The matter presented in this thesis has not been submitted by me for the award of any other degree of this or any other institute.

Sampurna Dasgupta

Signature of the student

(Sampurna Dasgupta)

This is to certify that the above statement made by the candidate is correct to the best of my/ourknowledge.

Signature of the Supervisor

(Dr. Sharad Gupta)

SAMPURNA DASGUPTA has successfully given his/her M.Sc. Oral Examination held on **May 9, 2023**.

Signature(s) of Supervisor(s) of MSc thesis
Date:

P.V. Kodgire
Convener, DPGC
Date:

Signature of PSPC Member
(Prof. Amit Kumar)
Date:

Signature of PSPC Member
(Dr. Abhijeet Joshi)
Date:

ACKNOWLEDGEMENTS

Completing this MSc thesis would not have been possible without the support, guidance, and encouragement of my supervisor **Dr. Sharad Gupta**. I take this opportunity to express my heartfelt gratitude to all those who have played a role in my academic journey. First and foremost, I would like to extend my sincere appreciation to my thesis guide for his invaluable guidance and support throughout this project. His expertise, insightful comments, and constructive feedback have been instrumental in shaping my research and in guiding me towards the right direction. I am grateful to him for his unwavering belief in my abilities and for his continuous encouragement throughout this journey.

I would also like to express my sincere thanks to the faculty members of the Department of Biosciences and Biomedical Engineering, Indian Institute of Technology, Indore, for their support and encouragement during my academic journey. The stimulating academic environment and the challenging coursework have been instrumental in developing my critical thinking and research skills. I am grateful to my professors for their inspiring lectures, insightful comments, and valuable feedback that have helped me grow as a researcher and as an individual. I would like to take this opportunity to thank **Prof. Prashant Kodgire** for giving me invaluable suggestions for my research work and guiding me to critically think and evaluate my experimental approaches. He has always encouraged me to achieve more and have faith in myself. I would also like to thank **Dr. Parimal Kar** for guiding me and helping me, his support has proved to be invaluable and incredibly helpful in my Masters. He always understood the career venture I wanted to choose Despite his busy schedule, he made himself available to clear even my small doubts. He has moulded me into a better person for life! I would also like to convey my gratitude towards, DPGC and HoD of BSBE department for giving me this chance to work independently. I would also like to thank **Dr. Debashish Nayak** for his support and his crucial suggestions and guidance during the project and for providing me with scientific insights during my project. I am inspired by his scientific attribute. I have learned so

much from him. He had always motivated me for best. I am indebted for his valuable career advice. I would also like to thank **Dr. Patidar** for helping mw with the samples required for my project. I am also grateful **to Ms. Mitali Dave** and **Dr. Ravinder**, **SIC** for guiding me how to use the highly valuable instruments like SEM and confocal Microscope. I am immensely grateful to **Dr. Shovan Majumder** for taking me under his guiding light and helping me with Raman spectroscopic data and for letting me use his lab set up Raman spectroscopy. I would like to thank **Mr. Aniket Chowdhury**, **Shri Nitin Kumar** and **Ms. Shivangi Verma** for their tireless help in executing my experiments.

Moreover, I would like to extend my sincere appreciation to my Lab mates who generously shared their time and knowledge, without whom this research would not have been possible. Their willingness to participate and to share their personal experiences and perspectives have been invaluable in shaping the research findings. I am so grateful to **Dr. Suman Bishnoi** and **Dr. Saumya Jaiswal** and **Mr. Pankaj Kumar** for helping me at each difficult moment. I would like to extend my heartiest thanks to **Miss Anusha Srivastava** for helping me out whenever I was at crossroads and helping me out with execution of my experiments. I would also like to thank **Mr. Badri Sahoo** whose experimental dealings have inspired me heavily and for helping me with planning my own experiments. I would also like to thank **Mr. Abhijeet Singh, Ms Kali Meena, and Ms. Priyanka Payal** for supporting me.

I am also grateful to my peers, friends, and family members for their love, support, and motivation during the ups and downs of my research. I would like to specially thank my father **Mr. Biswajit Dasgupta** for supporting me throughout my career. Their unwavering encouragement and support have been instrumental in keeping me motivated and focused. I would like to express my heartfelt thanks to my friends for their countless hours of brainstorming, discussions, and critiques, which have enriched my research and made the journey more enjoyable. I would like to acknowledge the financial support from DBT during my MSc program. Their support has been

instrumental in enabling me to pursue my academic goals and in facilitating my research.

Lastly, I would like to thank all the staff members of **the Department of Biosciences and biomedical engineering, Indian Institute of Technology, Indore** for their assistance, guidance, and support throughout my MSc program. Their support in administrative matters, technical assistance, and logistical support has been invaluable in facilitating my research. I am deeply grateful to all those who have contributed to my academic journey, both directly and indirectly. Your support, guidance, and encouragement have been instrumental in shaping my research and in enabling me to achieve my academic goals. Thank you all for being a part of my journey.

Sampurna Dasgupta

This thesis

is dedicated to

My family, friends and

my beloved Juniors

Abstract

Artificial insemination (AI) using cryopreserved semen is the most widely used method to accelerate the production of livestock population. Sperm selection is a crucial component of assisted reproductive methodologies which helps in sorting out dead and damaged sperms from viable fraction. The low conception rate associated with using cryopreserved semen can be attributed to cryodamage that lowers the sperm viability. The presence of dead and defective sperms in the semen population limits artificial insemination to be exploited efficiently. The competent removal of dead sperms before cryopreservation can significantly increase the conception percentage. This thesis discusses a novel approach of magnetically activated bovine sperm cell sorting to get an enriched eluent comprising majorly of healthy and live sperms, which can further be used for AI. Interaction between phosphatidyl serine moieties of dead sperms and Annexin-V microbeads in a magnetic environment have been incorporated to work out a protocol for the separation of dead spermatozoa. Co-staining with PI/Hoechst and fluorophore-conjugated Annexin V were then employed to visualize dead sperms via fluorescence microscopy. This is a simple, rapid and cost-effective method for live sperm enrichment post-thawing of cryopreserved semen. Optical Tweezer Raman spectroscopy (OTRS) for differentiating the X-Spermatozoa and the Y-Spermatozoa has not been reported. This novel approach helped us in obtaining Raman Spectrum from healthy live cells. This technique is staining free, non-invasive, and is significantly better than using FACS based sperm sorting.

Keywords: Sperm enrichment assay, Dead and live Assay, Phosphatidylserine, Annexin V, Annexin V conjugated microbeads, Raman Spectrum, Optical Tweezer Raman spectroscopy.

CONTENTS

LIST OF FIGURES

List of Tables **Page No.**

LIST OF ABBREVIATIONS

2PEM	2-photon excitation microscopy
AI	Artificial Insemination
CASA	Computer assisted sperm analyzer
CCD	charge-coupled device
CMOS	complementary metal oxide semiconductor
CR	Conception Rate
CW	Continuous wave
EDS	Energy-dispersive X-ray spectroscopy
FACS	Fluorescence activated cell sorter
FITC	Fluorescein isothiocyanate
FOV	Field of view
IONP	Iron oxide nanoparticle
MACS	Magnetic assisted cell sorter
MCT	Micro centrifugation tube
MNP	Magnetic nanoparticle
NF	Notch filter
OTRS	Optical tweezer Raman spectroscopy
PBS	Phosphate buffer saline
PI	Propidium Iodide
PMT	Photomultiplier tube
PS	Phosphatidyl serine
RPM	Rotation per minute
SEM	Scanning electron microscopy
STED	Science & Technology Entrepreneurship Development

Chapter 1

Introduction

Dairy industry around the globe has witnessed mushroom growth in terms of milk production and usage in past several decades [1]. Speculations about the rising consumption of dairy products suggests an increasing trend in compound annual growth rate (CAGR) of global dairy market. The CAGR of milk production (4.34 % p.a.) was found to be more in comparison to per capita availability (2.71 % p.a.) [2]. India being entitled as the "largest milk producer in the world" still holds great potential to augment milk production [3].

Artificial insemination (AI) is the globally used assisted reproductive technique for animal breeding and it has gone various modifications over the past six decades [4]. The primary workflow involved in animal breeding and milk production lies in the hand of small landholders and farmers who use unsorted semen to artificially inseminate the cattle [5]. Sperms collected from bovine are subjected to cryopreservation for storage and transport. The cryopreservation which involves freezing and thawing of semen sample causes physiological damage to a major chunk of spermatozoa which remain suspended along with the live fraction [6].

The commercial success of dairy farming depends upon the efficiency of the conception rate of artificial insemination methods. There exists documented evidence about the presence of dead and defective sperms in cryopreserved semen that eventually contributes to inefficient insemination and low conception efficiency [7]. Separating dead and damaged sperm cells from live fractions can significantly improve the conception rate [8]. Hence, there exists a dire need to remodel conventional AI techniques.

Various methodologies have surfaced for sperm sorting before proceeding with AI. Among them are flow cytometry, swim-up procedure coupled with quantification, microfluidic based sorting etc. [9-12]. This study aims to develop a magnetic nanoparticles-based strategy to separate the dead and damaged sperms from the bovine semen samples using simple steps. To

address this issue, we are incubating bovine semen samples with the magnetic annexin-V conjugated microbeads in a strong magnetic field [13]. The Annexin-V conjugated magnetic microbeads bind to phosphatidylserine that is expressed on the surface of dead and defective sperms [14, 15]. In the presence of the strong external magnetic field, all the dead and defective cells are trapped and viable sperm cells can be collected [16]. In this manner, we get a population of sperm that are viable and live. This healthy fraction of sperm samples can be used in artificial insemination to obtain a higher conception rate in cattle for increased milk productivity [17].

1.1 Importance of Sperm Sorting

Semen sexing in bovine reproduction is a powerful tool that has been extensively researched and developed over the past few decades. The technology relies on differences in the physical and genetic characteristics of X and Y chromosome-bearing sperm cells, which can be separated and sorted using flow cytometry or microfluidic devices [18, 19].

One study published in the Journal of Dairy Science in 2014 evaluated the effects of using sexed semen on dairy herd genetics and economics. The researchers found that using sexed semen to increase the number of female offspring produced resulted in a decrease in the effective population size of the herd, which could lead to a reduction in genetic diversity over time. However, the use of sexed semen also led to increased milk production and higher profitability for the dairy farmers. The authors suggested that a balance between genetic improvement and maintaining genetic diversity should be considered when using semen sexing in dairy cattle.

Another study published in the Journal of Theriogenology in 2020 compared the fertility and pregnancy rates of heifers inseminated with sexed and non-sexed semen. The researchers found that the conception rates were lower for sexed semen than non-sexed semen, but the pregnancy rates were similar for both groups. The authors suggested that the use of sexed semen in heifers may require adjustments to breeding management, such as using higher doses of semen or more frequent inseminations, to optimize fertility rate.

However, in beef cattle, the use of sexed semen has been shown to increase the proportion of male calf produced, which can have economic benefits for the industry. A study published in the Journal Animal in 2021 evaluated the use of sexed semen in a beef cattle population and found that it led to an increase in the proportion of female calves born and an improvement in the genetic quality of the herd. The authors suggested that the use of sexed semen in beef cattle production can be an effective tool for improving the profitability and sustainability of the industry.

1.2 Advantages of semen sexing

While the use of semen sexing technology has several advantages, it also raises important ethical and scientific considerations, such as the potential impacts on genetic diversity and animal welfare. A review published in the journal Theriogenology in 2017 evaluated the impacts of semen sexing on genetic diversity in livestock populations. The authors found that the use of semen sexing can lead to a reduction in genetic diversity if the technology is used extensively to select for specific genetic traits. They suggested that the use of semen sexing should be balanced with other breeding strategies to maintain genetic diversity in livestock populations.

With the use of artificial insemination (AI) becoming increasingly popular in livestock breeding, advancements in semen sexing technology have led to a variety of benefits. One of the main advantages of semen sexing technology is the ability to control the sex ratio of offspring, which has significant economic implications for livestock production.[20]–[22] By selectively inseminating females with either X or Y sperm, breeders can ensure the birth of offspring of a desired sex. In the cattle industry, where farmers typically strive for a higher percentage of heifers to replace their milk-producing mothers, semen sexing technology has proven especially useful. Accurate sexing also allows for the selection and breeding of superior genetics, which in turn leads to improved productivity and profitability. It is worth noting that while semen sexing technology has been largely successful in cattle breeding, its application in other livestock industries varies. Moreover, X-sorted sperm technology provides further advantages. X-sorted

sperm technology enables breeders to increase the proportion of female offspring produced. This is particularly useful in animal breeding programs where females are preferred for their milk or meat production. In addition to the benefits of controlling sex ratio in livestock production, semen sexing technology has other advantages as well [14].

In conclusion, the use of semen sexing in bovine reproduction has been extensively researched and developed, and has been shown to have significant economic benefits for both dairy and beef cattle production. However, careful consideration of its impacts on genetic diversity and animal welfare is necessary, and its use should be balanced with other breeding strategies to ensure the long-term sustainability of the industry.

1.3 Conventional techniques used for semen sorting

Prior to the development of flow cytometry and microfluidics, there were several conventional methods for bovine semen sexing, although these methods were generally less effective and more labour-intensive. These included cell morphology analysis and cell motility and percoll density gradient and swim up techniques [9]. One conventional method for semen sexing in bovine reproduction was based on the principle of sperm cell motility. X chromosome-bearing sperm cells were believed to swim slower than Y chromosome-bearing sperm cells due to their larger size and more complex genetic structure. As a result, semen samples were subjected to a centrifugation process that separated the slower-swimming X chromosome-bearing sperm cells from the faster-swimming Y chromosome-bearing sperm cells. However, this method was not very reliable, and often resulted in low pregnancy rates.

Another conventional method for semen sexing in bovine reproduction was based on the principle of sperm cell morphology. X chromosome-bearing sperm cells were believed to have a more oval-shaped head than Y chromosome-bearing sperm cells, which had a more pointed head. As a result, semen samples were subjected to a staining process that allowed for the visual identification of X and Y chromosome-bearing sperm cells based on their head shape. However, this method was also not very reliable, and often

resulted in low pregnancy rates. Percoll density gradient is a technique used to separate sperm cells based on their density. In this method, a gradient of Percoll, a solution with a high density, is prepared in a centrifuge tube. Semen samples are layered on top of the gradient and centrifuged. The centrifugation process separates the sperm cells based on their density, with the X chromosome-bearing sperm cells settling at the bottom of the tube and the Y chromosome-bearing sperm cells settling towards the top [26]. The separated sperm cells are then collected and used for artificial insemination. However, this method is less effective and more labour-intensive than flow cytometry or microfluidics, and is rarely used in modern bovine reproduction [16].

Sperm swim-up is another conventional method used for bovine semen sexing, which separates sperm cells based on their motility [27]. In this method, semen samples are placed in a tube containing a culture medium, and incubated for a short period of time. The faster-swimming Y chromosome-bearing sperm cells are believed to swim up to the surface of the medium more quickly than the slower-swimming X chromosome-bearing sperm cells [28]. The surface layer of the medium is then collected and used for artificial insemination. However, this method is also less effective and more labour-intensive than flow cytometry or microfluidics, and is rarely used in modern bovine reproduction.

The development of flow cytometry and microfluidics has largely replaced these conventional methods for bovine semen sexing, as they are more accurate, reliable, and efficient. However, these older methods played an important role in the early development of semen sexing technology, and paved the way for the more advanced techniques that are used today. While these conventional methods have been largely replaced by more advanced technologies, they played an important role in the early development of semen sexing technology, and may still be used in certain situations [29] where flow cytometry or microfluidics are not available or practical.

1.4 Current methods of bovine semen sexing: flow cytometry and microfluidics

Flow cytometry is a commonly used method for semen sexing in bovine reproduction. This method relies on the physical and genetic differences between X and Y chromosome-bearing sperm cells, which can be separated and sorted based on their fluorescence properties. Sperm cells are stained with a fluorescent dye that binds to their DNA, and the cells are then passed through a flow cytometer, which detects and sorts the cells based on their fluorescence properties. X chromosome-bearing sperm cells are generally larger and have more DNA than Y chromosome-bearing sperm cells, and therefore appear as distinct populations in the flow cytometer. The sorted sperm cells are then collected and used for artificial insemination [23].

Microfluidics is a newer method for semen sexing in bovine reproduction that involves the use of microchannels and microstructures to sort sperm cells based on their size, shape, and/or electrical properties [24]. Microfluidic devices can sort sperm cells at higher speeds and with greater accuracy than flow cytometry, and can also be used to select sperm cells based on their motility or other functional characteristics. Microfluidics can also be used for single-cell analysis, which allows for the detection and selection of specific sperm cells with desirable genetic traits. However, microfluidics is a more complex and expensive method than flow cytometry, and requires specialized equipment and expertise [25].

Both flow cytometry and microfluidics have their advantages and disadvantages in bovine semen sexing, and the choice of method will depend on various factors, including the desired sex ratio of offspring, the genetic traits being selected for, and the available resources and expertise. While semen sexing technology has revolutionized the bovine reproduction industry, it is important to carefully evaluate the impacts of its use on genetic diversity and animal welfare, and to use it in conjunction with other breeding strategies to ensure the long-term sustainability of the industry.

1.5 Aim of the Project

The conception rate (CR) in bovines are about 33 % which leads to decrease in the pregnancy rates in bovines, to cater to this problem we need to remove the dead and defective sperm cells from the sample population. The primary aim of the thesis is to remove the dead and defective sperm cells from the entire population of semen sample. Thus, making the healthy and motile sperm cells available for artificial Insemination (AI). So, the expected outcome is that when these sorted cells are used for artificially inseminating the bovines, the conception rate should increase significantly.

The second aim of the thesis is the identification of X-chromosome containing spermatozoa in the sample population which contains equal proportion of X-spermatozoa and Y-spermatozoa. This will enable us to have a skewed population of sperm cells which mostly contains X-spermatozoa. When this skewed population of sperm cells are used for artificially inseminating the bovines, the probability of conceiving a female calf will be more than that of a male calf.

Chapter 2

Materials and Methods

Separation of the dead and defective spermatozoa from the entire semen sample

2.1 Chemicals and kits

The Annexin V Microbead kit was purchased from the Miltenyi Biotec (Germany). The Annexin V-FITC Apoptosis detection kit and Propidium Iodide dye was bought from the Sigma-Aldrich (USA). Stock solutions were stored in amber-coloured microcentrifuge tubes (MCT) at 4 °C temperature for further use. 1 X PBS buffer containing 137 mM NaCl, 2.7 mM KCl, 10 mM Na_2HPO_4, and 1.8 mM KH_2PO_4 was prepared, and the required pH 7.0 was achieved with the help of HCL and NaOH. The exact amounts are depicted in table 2.1. PBS was selected as a buffering agent for its wide buffering range and because it contained NaCl, hence could provide a pH very close to physiological pH.

Table 2.2: Ingredients of 1 X PBS buffer

*C*omponent	Quantity added *(gram)*
KH_2PO_4	313.5
Na_2HPO_4	1.42
NaCl	8.0
KCl	201.2

Semen straws were obtained from a veterinary doctor near the institute. The semen sample comes in a slender tube or a straw. The straw has one end sealed and the other plugged with cotton. Figure 2.1 shows the different sections of conventional semen straws, after collection of the semen the processed semen is packed into such straws.

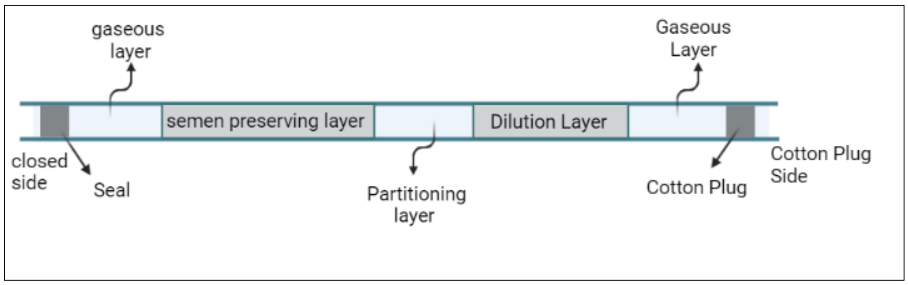

Fig. 2.1: Schematic of different sections of the conventional semen straw

2.1.1 Annexin V

Annexin V is a protein that has a high affinity for phosphatidylserine, a phospholipid that is typically found in the inner leaflet of the plasma membrane of healthy cells. However, when a cell undergoes apoptosis (programmed cell death), phosphatidylserine becomes exposed on the outer surface of the plasma membrane. Annexin V is commonly used in biomedical research to detect apoptosis. By labeling annexin V with a fluorescent tag, researchers can detect and quantify the number of apoptotic cells in a population [30]. This technique is commonly used in studies of cancer, where it can be used to evaluate the efficacy of chemotherapy or radiation therapy. It is also used in studies of neurodegenerative diseases, such as Alzheimer's disease, where apoptosis plays a key role in disease progression. Figure 2.2 shows the structure of the Annexin V protein.

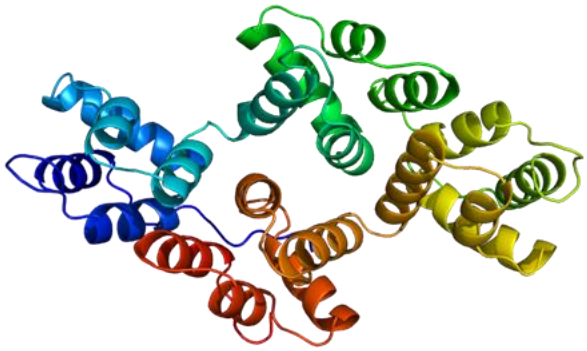

Fig. 2.2: The structure of Annexin V protein (PubMed ID-8254674)[31].

2.1.2 Annexin V-FITC

Annexin V-FITC is a widely used fluorescent probe that is used to detect apoptotic cells. It is a conjugate of annexin V protein and a fluorescein isothiocyanate (FITC) fluorescent dye. When annexin V-FITC binds to

phosphatidylserine that is exposed on the outer surface of apoptotic cells, it can be detected by fluorescence microscopy or flow cytometry [32, 33]. The use of annexin V-FITC in combination with a propidium iodide (PI) stain is a common technique for distinguishing between early and late-stage apoptotic cells. PI is a fluorescent dye that cannot penetrate the membrane of viable or early apoptotic cells, but can penetrate the membrane of late-stage apoptotic cells with compromised membranes or necrotic cells. Therefore, cells that are Annexin V-FITC positive and PI negative are in the early stages of apoptosis, while cells that are Annexin V-FITC positive and PI positive are considered to be in the late stages of apoptosis or necrotic. Annexin V-FITC staining is a reliable and sensitive technique for detecting apoptotic cells, and it is commonly used in research studies and diagnostic applications.

2.1.3 Propidium Iodide (PI)

Propidium Iodide (PI) is a fluorescent intercalating dye (its chemical structure shown in Fig. 2.3) commonly used in biological research to stain and identify dead cells. PI can be used to distinguish between live and dead cells based on the integrity of their cell membranes. PI is unable to cross the intact membrane of live cells but can penetrate the membrane of dead or dying cells, intercalate with DNA, and fluoresce upon binding to double-stranded DNA.

PI is often used in combination with other fluorescent probes, such as Annexin V-FITC, to differentiate between different stages of cell death. For example, Annexin V-FITC can detect early-stage apoptotic cells that have externalized phosphatidylserine, while PI can detect late-stage apoptotic cells or necrotic cells with compromised membranes. By using both probes in combination, researchers can identify and quantify different stages of cell death in a sample.

PI staining is also commonly used in flow cytometry, a technique that allows for the high-throughput analysis of individual cells in a heterogeneous population. In flow cytometry, PI staining can be used to identify dead cells in a sample, enabling the exclusion of these cells from subsequent analysis.

Overall, PI staining is a useful tool for identifying and quantifying dead cells in a variety of research applications, including cell culture, tissue analysis, and diagnostic assays.

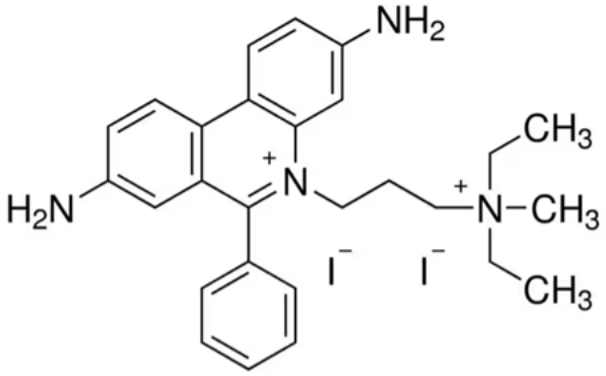

Fig. 2.3: Chemical structure of Propidium Iodide [34].

2.1.4 Hoechst stain

Hoechst 33342 is a fluorescent dye (its chemical structure is shown in Fig. 2.4) that specifically binds to DNA through minor groove interactions, rather than intercalation. The dye's fused aromatic rings can form hydrogen bonds with the DNA backbone, while its tertiary amine groups can form hydrogen bonds with the bases of the DNA. These interactions allow Hoechst 33342 to specifically bind to AT-rich regions of DNA, which have wider minor grooves than GC-rich regions [35].

The absorption spectrum of Hoechst 33342 has a peak at around 350 nm and a shoulder at around 450 nm. The dye absorbs strongly in the ultraviolet (UV) region, with a molar extinction coefficient of around 60,000 $M^{-1}cm^{-1}$ at 350 nm. The emission spectrum of Hoechst 33342 has a peak at around 460 nm and a shoulder at around 540 nm. The dye emits blue fluorescence when it is excited by UV light, with a quantum yield of around 0.8 in aqueous solution. The emission maximum can shift to longer wavelengths (up to 485 nm) when Hoechst 33342 is bound to DNA [36]. The specific spectral properties of Hoechst 33342 can vary depending on factors such as solvent environment, pH, and binding to DNA or other biomolecules. However, the absorption and emission spectra are commonly used to excite and detect Hoechst 33342 fluorescence in imaging and spectroscopy applications [37].

Once Hoechst 33342 is bound to DNA, it undergoes a conformational change that results in a significant increase in fluorescence. This fluorescence is due to the formation of an excited-state dimer, which occurs when two dye molecules are near each other. The dimer emits blue light when it returns to its ground state, and this emission is used to visualize the presence and location of DNA in cells and tissues. Hoechst 33342 is commonly used in cell biology and biochemistry research to label DNA and study cell division, migration, apoptosis, and other cellular processes.

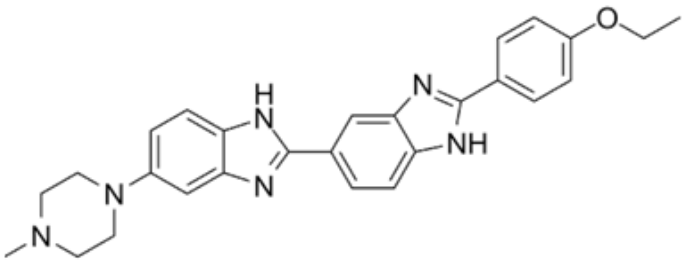

Fig: 2.4: Chemical structure of Hoechst 33342 [38].

However, Hoechst 33342 has several derivatives that differ in their chemical structure, binding specificity, fluorescence properties, toxicity, and cell permeability. Hoechst 33258, for instance, has a similar structure to Hoechst 33342 but with only one benzene ring, and it prefers to bind to GC-rich regions of DNA. Hoechst 34580, on the other hand, has a dibenzofuran structure and a higher fluorescence quantum yield than Hoechst 33342 [39]. Hoechst 33342 trihydrochloride has a similar structure to Hoechst 34580 but with a different chloride counterion, and it has higher cell permeability than Hoechst 33342. The choice of Hoechst 33342 derivative depends on the specific experimental conditions and research question, as each derivative has unique properties that may be advantageous or disadvantageous for certain applications.

2.2 Semen Processing

Frozen semen straws were obtained from various different breeds like the Jersey bulls, Holstein Friesian bulls, Sahiwal and Holstein Friesian cross were stored in liquid nitrogen at -196 °C. The sample initially contains a lot of protein and cell debris which needs to be removed to obtain a more

repeatable starting point. The semen straws also contain cryoprotectant and freezing media, in order to remove those components, we centrifuge the sample. To accomplish this, the semen sample is emptied into a 2 ml MCT tube and 1 ml of Phosphate Saline Buffer was added to it. It was then given a short mini spin for 2 minutes at 1000 RPM to remove the debris. The supernatant was aliquoted in another fresh MCT and centrifuged at 300 G for 10 minutes. The supernatant was discarded and the pellet was dissolved in 500 µl of PBS and kept on ice for further experiments.

2.3 Sperm Counting

The sperm concentration was determined by using a hemacytometer, 10 µl of spermatozoa were loaded on the hemacytometer and were visualized under CASA (Computer Assisted Sperm Analyzer) which is equipped with a stage warmer that can be adjusted to 25 °C. All 4 corners of the hemacytometer were counted and a video of each square was recorded individually. The number of motile sperms was also counted in each square and an average ratio was obtained of the percentage of motile sperms in the entire sample.

2.4 Motility analysis by phase contrast microscopy

2.4.1 Temperature dependent analysis

To provide quantifiable proportions of live and dead spermatozoa, the CASA was utilized to determine motility percentage at two different temperatures: 4 °C and room temperature, 25 °C. After the thawing of sperms, the cells were divided into two parts, one part was maintained at 25 °C and the other part was maintained at 4 °C. both the samples were centrifuged at 300G for 10 minutes and the pellets were suspended in PBS. 10 µl of each sample was mounted in a hemacytometer for motility analysis under a Phase contrast microscope (Leica DM1000 LED under magnification 40X and phase ring adjusted at PH 2) and the stage warmer was set at respective temperatures to maintain the temperature throughout the counting process. All 16 squares of each corner were counted and the motility percentage was found at both temperatures.

2.4.2 Time dependent analysis

To understand till what time the cell retains its viability and motility we performed an analysis where we checked the viability of the sperm cells at 5 different time points. After pre-processing the semen sample the sample was resuspended in 1000 µl 1 x PBS. In five different MCT (T= 0 min, T= 10 min, T= 20 min, T= 30 min, T= 60 min), 200 µl of semen sample solution was aliquoted. After the respective time periods were over, Propidium Iodide was added to all the MCTs and incubated for 3 minutes and then centrifuged at 300 G for 10 minutes. The pellets were dissolved in 100 µl 1 x PBS and observed under fluorescence microscope.

2.5 Magnetic labelling of sperms using Annexin V conjugated microbeads and live-dead cell sorting

A fresh semen straw was thawed at 37 ˚C for 3 minutes. The cells were washed with 1× PBS (1000 µL) by centrifugation at 300 g for 5 minutes. Cells were counted using a hemocytometer and ~10^6 cells were taken for further experiments. The cell suspension was centrifuged at 300 G for 10 minutes and the cell pellet was resuspended in 80 µL of 1× Binding Buffer. 20 µL of Annexin V MicroBeads was added per 10^7 cells and incubated for 15 minutes in the refrigerator (2−8 ˚C). All the steps were carried out in dark. Sperm cells were washed using 1 – 2 ml of 1 x binding buffer and centrifuged at 300 g for 10 minutes and then the cells were resuspended in 500 µL of 1× binding buffer.

For sorting of dead and live cells, the sperm-microbead suspension was loaded on the separation column which is fitted with neodymium magnets. The separation column is devised in such a way that the distance between the column wall and the neodymium magnets is not more than 2 mm. The opening at the bottom of the column is sealed with a cap so that it stops the solution from flowing out. The cell suspension was carefully loaded onto the column in a dropwise manner and incubated for 5 minutes. After the incubation time, the cap is removed and the eluent was collected in a fresh MCT. The eluted cells were stained with PI (working solution 0.1 mg/ml) dye

for 5 minutes and then washed with 1× PBS (250 µL) and then centrifuged at 300 G for 5 minutes to remove the excess PI dye. In order to confirm the results of the experiment the same sample was stained with Annexin V–FITC. The cells were visualized under a fluorescence microscope. Figure 2.5a shows the image of the magnetic activated cell sorter column, which is fitted with a long column of neodymium magnet and Fig. 2.5b shows the actual set up that is being used for the magnetic activated cell sorting. The set up that is being used for the sorting is indeed very simple and the process is easy to perform, it includes a 3 ml syringe tube with its mouth capped so that the sample can be incubated within it. Inside the syringe neodymium magnets are stacked up to form a cylinder like structure. The magnets are of such a size that it only leaves a gap of few millimetres between the wall of the syringe and the neodymium magnets.

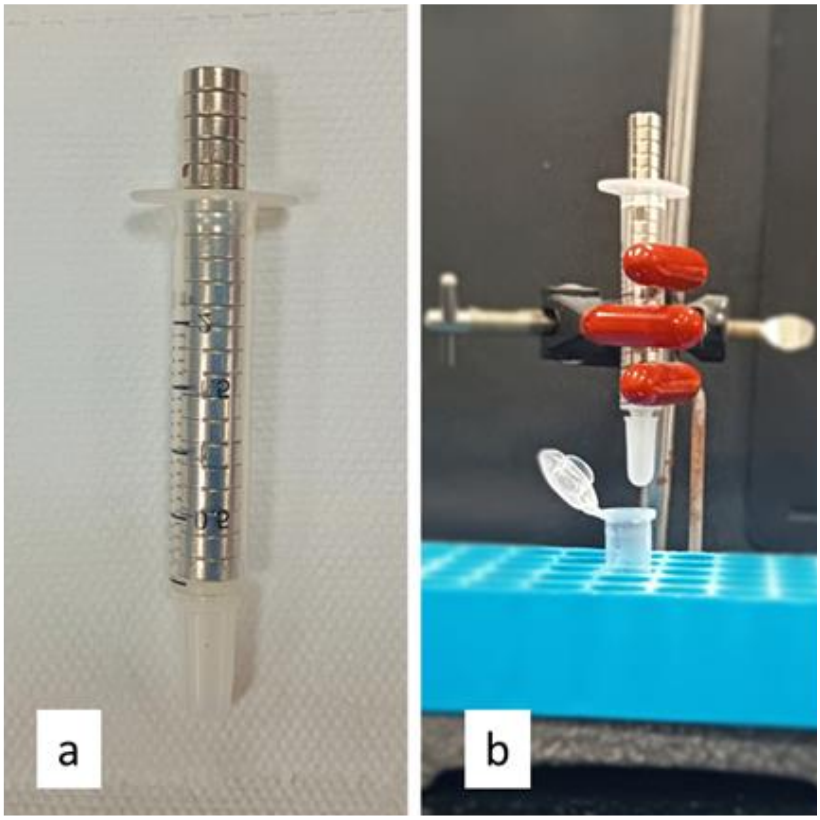

Fig. 2.5: (a) image of the magnetic activated cell sorter column and (b) the actual set up used for the magnetic activated cell sorting.

2.6 Live and dead sperm detection before and after enrichment assay

2.6.1 Propidium Iodide and Annexin V- conjugated FITC

To assess sperm viability after the enrichment assay, the eluted fraction was stained with Propidium Iodide and was analyzed using a fluorescent microscope (Nikon eclipse Ti-U) loaded with triple filters. 10 µl of Propidium Iodide (working concentration-1mg/ml) was added to the eluted semen fraction and was incubated in dark over ice for 3 minutes. The same cells were then stained with Annexin – V conjugated FITC which would fluoresce green when it binds to Phosphatidylserine. 5 µl of Annexin V-FITC was added to 100 µl of semen sample and incubated for 10 minutes. Followed by incubation, the samples were centrifuged at 300G for 10 minutes, and the pellet was resuspended in 1X PBS. 10 – 20 µl of the sample was pipetted on a clean slide and covered with a 22 x 22 mm cover glass and was observed under 40X magnification. Bright-field images along with fluorescent images of the same field of view were captured. Experiments were done in triplicates and a minimum of 200 spermatozoa were counted for the experiments.

2.6.2 Cell staining using Propidium Iodide

The eluted spermatozoa suspension was centrifuged at 300 G for 10 minutes and the pellet was resuspended in PBS. 100 µl of the sample was aliquoted in a fresh MCT. 10 µl of Propidium Iodide was added (working solution 0.1 mg/ml) was added to it and the MCT was incubated for 3 minutes. For Fixing the cells, 15 µl of 2 % paraformaldehyde was added to the tube and incubated for 2 minutes on ice. 500µl of PBS was added to wash the cells and centrifuged at 300 G for 10 minutes. The pellet was resuspended in 100 µl PBS. For obtaining a clear image we fixed the positions of the cover slip with glycerol. 20 µl of the sample was loaded onto a circular glass coverslip (14mm diameter) and air dried. 5 µl of 70 % glycerol was added to the clean glass slide and the air-dried cover slip was carefully inverted on top of it creating a sealed frame. The cells were visualized under 40 x magnification under a fluorescence microscope.

Identification of the X chromosome containing spermatozoa from the live fraction of the semen sample

2.7 Cell sorting by Optical Tweezer Raman Spectroscopy (OTRS)

2.7.1 Sample preparation for OTRS

The Unsorted cell sample and the sorted sample was prepared individually. The semen straws were emptied into a 2 ml MCT tube and 1 ml of Phosphate Saline Buffer was added to it. It was then given a short mini spin for 2 minutes at 1000 RPM to remove the debris. The supernatant was aliquoted in another fresh MCT and centrifuged at 300 G for 10 minutes. The supernatant was discarded and the pellet was dissolved in 500 µl of PBS and kept on ice for further experiments.

2.7.2 Optical Tweezer Setup and Sperm Cell Trapping

Optical tweezer system was set up with a trapping laser beam (1064 nm) that is focused on a small area in the sample. Majorly the laser beam was focused on the head of the sperm cells, approximately where the nucleus is situated. The Raman probe laser was set a wavelength of 532 nm. Using the optical tweezers, individual sperm cells were trapped in the laser beam. This can be achieved by adjusting the position and intensity of the laser beam to create a trapping potential that holds the cell in place. Around fifty individual sperms were trapped individually and analyzed. Once the cells are trapped, Raman spectroscopy was used to analyze its biochemical composition. The laser beam should be focused on the cell to collect Raman scattering from the different components of the cell.

2.8 Instrumentation

2.8.1 Fluorescence Microscopy

Fluorescence microscopy is an important tool for studying cell physiology. It is intended to improve spatial resolution and picture contrast, and it can be customized to target proteins, lipids, or ions. It is nevertheless constrained by physical factors, resolution being the most significant one.

The basics of wide-field microscopy are outlined to emphasize the selection, advantages, and correct use of laser scanning confocal, two-photon, scanning disc confocal, total internal reflection, and super-resolution microscopy [43, 44]. Recent fluorescent microscopy improvements have attempted to increase image quality by tackling the underlying problem of image resolution. The ECLIPSE Ti-U inverted microscope (image is shown in Fig. 2.6) has an unprecedented 25mm field of vision (FOV) [45]. The Ti-U maximizes the sensor area of large-format CMOS cameras without sacrificing data speed, thanks to its excellent field of view. The Ti-U has an extremely stable and drift-free architecture which gives super-resolution imaging, while its unique hardware-triggering features improve even the most difficult, high-speed imaging applications. Furthermore, by gathering data from internal sensors, the Ti2's unique, intelligent functionalities guide users through imaging workflows, eliminating the risk of user error. Furthermore, throughout acquisition, the state of each sensor is automatically recorded, enabling quality control for imaging investigations and improving data repeatability [46].

Fig. 2.6: Image of the ECLIPSE Ti-U inverted fluorescence microscope.

2.9 Raman Spectroscopy and OTRS

Raman spectroscopy is a powerful analytical technique used for the characterization of materials. The principle behind Raman spectroscopy is based on the inelastic scattering of light by molecules, which results in a

shifted spectral pattern known as the Raman Effect. This effect occurs when a photon interacts with a molecule and transfers energy, causing the molecule to enter an excited vibrational state. The Raman spectroscopy method works on the principle of inelastic scattering of monochromatic light from a laser beam [52]. When the laser beam illuminates a sample, electrons absorb photons' energy and become excited, resulting in an inelastic scattering of monochromatic light due to the interaction between incident photons and electrons. This scattered light has a different frequency than incident light and is used to derive valuable information on the sample's chemical structure, electronic configuration, and molecular bonds. This non-invasive and label-free technique has a wide range of applications in various fields such as chemistry, biology, material science and engineering. [53]

Raman spectroscopy typically includes several components that are necessary for the measurement process. In most cases, a laser is used as the source of monochromatic light, which interacts with the sample and induces Raman scattering. The scattered light from the sample is then analyzed using a spectrometer to detect its frequency shift relative to the incident laser beam.

2.9.1 Raman Optical Tweezer

Raman optical tweezers involves recording of Raman spectra from optically trapped biological cells. Figure 2.7 depicts the schematic diagram of OTRS. The technique being non-contact in nature causes minimal perturbation to cells under investigation, and offers improved signal to noise ratio for the spectra. The 532 nm continuous wave (CW) beam from a frequency doubled Nd: YVO4 laser (Verdi −5; Coherent Inc., Santa Clara, California) was used for exciting the Raman spectra. Through the illumination condenser (Numerical Aperture, NA 0.55) the laser beam was introduced into the sample chamber placed on a commercial inverted microscope (Axiovert 135TV; Carl Zeiss AG, Germany) and the Rayleigh scattered laser light and Raman scattered light were collected by a 60×, 1.35 NA microscope objective lens. The light was then passed through a notch filter to reject the Rayleigh scattered light and the Raman signal after the filter was coupled to an imaging spectrograph (Shamrock SR-303i; Andor Tech.,

UK). Raman spectra were recorded from single sperm cells by trapping and manipulating the cell into the 532 nm laser beam with the help of a laser trap formed using the 1064 nm beam [58]. For recording spectra, the cells were placed on the bottom surface of the sample chamber in path of the 532 nm laser beam. Two sets of semen sample were collected from the veterinary doctor and stored in liquid nitrogen at -196°C. Sorted and unsorted semen samples were then preprocessed by dissolving the semen into 1000 µl PBS and spinning it in a mini spin for 3 minutes at 1000 RPM. The supernatant was collected and aliquoted in a fresh mini centrifuge tube, it was then centrifuged at 300 G for 10 minutes. The pellet was dissolved into PBS and the supernatant was discarded. The palette was then diluted in 2 µl PBS. The cell suspension was mixed thoroughly by pipetting and a 5 µl drop was casted on the slides that were prepared for Raman. The slides which were used were not just simple glass slides. They were created by sandwiching covers slips on top of thin glass slides with the help of double tape. Two thin double tapes were pasted in between the glass slides and the cover slips so that it can create a gap of few micrometers. The sample were loaded on to these fine gap sutures and observed under the microscope.

Positioning of the cells into the 532 nm laser beam. The typical time required for positioning the cells were about 5-15 seconds and during that time 532 nm laser was kept blocked. The 532 nm laser spot size at the focus was approximately 15 µm and therefore could illuminate and excite spectra from the head of the cell. Since the cells are motile in nature the optical tweezers helped in trapping the cells to ensure that only one cell is illuminated at a time by the 532 nm laser beam. The 532nm laser and the optical trap (1064 nm laser) are coupled to the sample using a silver mirror through the condenser and the objective lens respectively. The Raman signal was observed via a spectrograph-CCD system after rejecting the elastically scattered light by using a notch filter (NF). To allow observation of the trapped sperm cells a halogen illumination source and a video CCD camera were used.

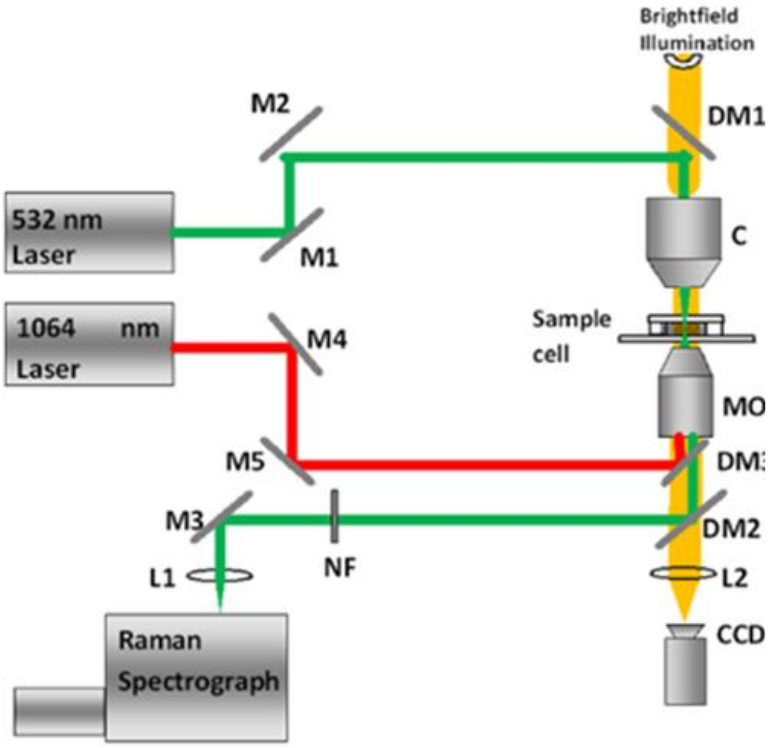

Fig. 2.7: Schematic of the experimental set-up of the OTRS.

2.10 Scanning electron microscopy

Scanning Electron Microscopy (SEM) is a technique that allows for the imaging of surfaces at high resolution using an electron beam. Figure 2.8 demonstrates the schematic diagram of SEM machine and its components. The principle of SEM is based on the interaction between a beam of electrons and the sample surface. The electrons interact with the atoms in the sample, producing various signals that can be detected and used to form an image. The electrons used in SEM are typically accelerated to energies between 1 and 30 keV. The electron beam is focused onto the sample surface using a series of magnetic lenses, and the sample is placed in a vacuum chamber to avoid scattering of the electrons by air molecules. When the beam strikes the sample, it produces a range of signals, including secondary electrons, backscattered electrons, and characteristic X-rays.

Secondary electrons are low-energy electrons that are emitted from the surface of the sample when it is struck by the primary electron beam. These electrons are used to form the SEM image, and provide information about the surface morphology of the sample. Backscattered electrons are high-energy

electrons that are reflected from the sample surface, and are used to provide information about the sample's composition and density. Characteristic X-rays are produced when the primary electrons knock out inner-shell electrons from the atoms in the sample. The energy of these X-rays is characteristic of the element from which they were emitted, allowing for elemental analysis of the sample. SEM can provide high-resolution images of the sample surface, with resolutions ranging from a few nanometers to tens of nanometers. The technique is widely used in materials science, nanotechnology, and biology to study the structure and properties of materials at the nanoscale. It is particularly useful for the study of surface morphology, particle size, and composition of materials.

Scanning Electron Microscopy (SEM) consists of several parts that work together to generate high-resolution images of the surface of a sample. Here are some of the main parts of an SEM:

1. Electron Gun: This part generates a beam of electrons that is focused onto the sample surface.
2. Electron Lenses: A series of magnetic lenses that focus and shape the electron beam to achieve high resolution imaging.
3. Sample Chamber: This is a vacuum chamber where the sample is placed during imaging to avoid scattering of the electrons by air molecules.
4. Sample Stage: The sample is mounted on a stage that can be moved in different directions to allow for imaging from different angles.
5. Detectors: There are several types of detectors that can be used in SEM, including secondary electron detectors, backscattered electron detectors, and X-ray detectors. These detectors detect the signals produced by the interaction of the electron beam with the sample and convert them into an image.
6. Control and Display System: This is a computer system that controls the SEM and displays the images obtained during imaging.

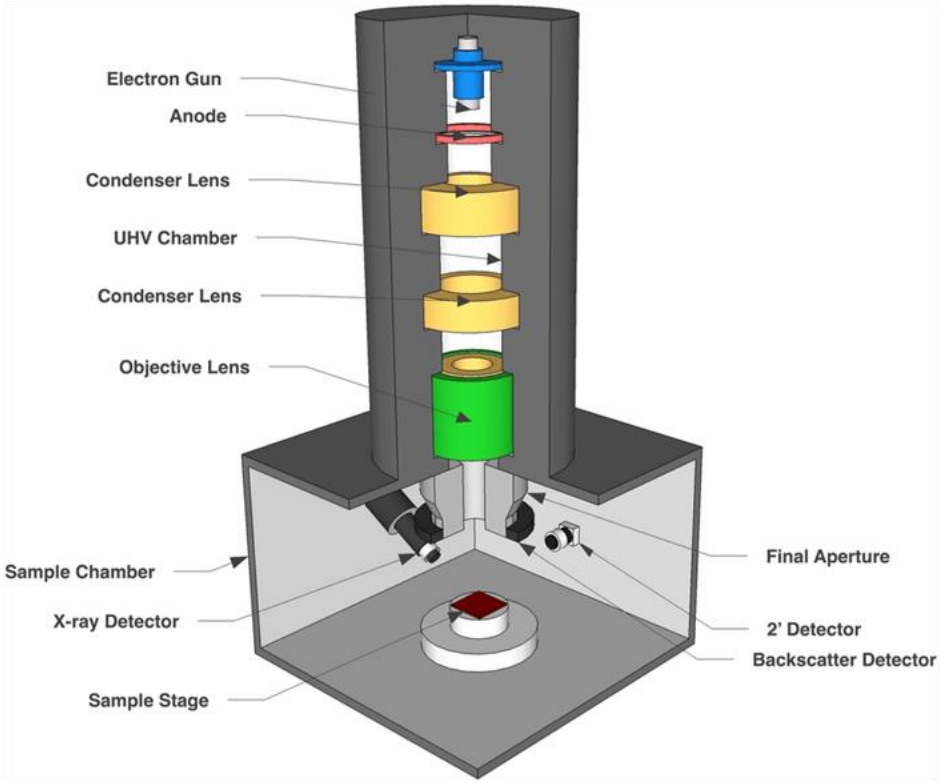

Fig. 2.8: Schematic of SEM machine and its components.

Chapter 3

Results and Discussion

In this study, we have devised a new approach to sort the live and dead sperm cells from the sample population in order to obtain a population with a relatively much lesser number of dead cells. Figure 3.1 shows the phase contrast image of a freshly thawed semen sample. The encircled areas of the image shows the presence of debris and dead cells. The presence of dead cells and debris might be responsible for the poor conception rates in bovines. This primarily happens because the debris present in the semen sample hinders the movement of the motile sperm cells. Motility is an essential factor for sperm to reach and fertilize the egg. If a significant portion of the sperm in the sample is dead, it may impede the sperm's ability to swim effectively towards the egg. The main aim is to obtain high-quality semen sample with a sufficient number of healthy, motile sperm to maximize the chances of conception in livestock. In order to clear out the debris in the semen sample the samples were given a short spin followed by centrifugation. The short spin will remove all the epithelial cells and other debris present in the sample and the centrifugation will remove the cryoprotectant and other toxic media components that were used in the media for preservation of the cells.

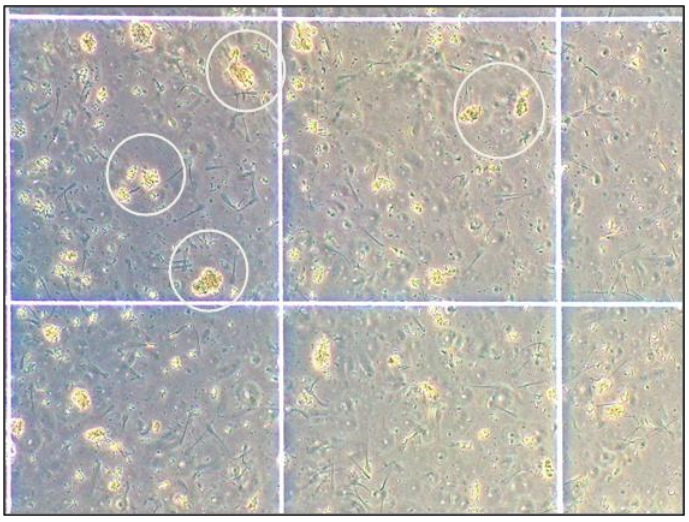

Fig. 3.1: Observed debris and epithelial cells found in the unsorted semen sample visualized using phase contrast microscopy (40X magnification). The encircled areas depict the debris present in the sample.

3.1 Motility analysis by phase contrast microscopy

To understand to what extent the cells retain its motility, temperature and time dependant motility analysis were performed. Figure 3.2 shows the sperm motility observed under two different incubation temperatures which is estimated by phase contrast microscopy.

Table 3.1*: The respective percentage motility of sperms incubated at 4 °C and 25 °C at five different time points.*

	T = 25 °C	T = 4 °C
t = 0 min	81.8 ± 4.04 %	79 ± 4.34 %.
t = 60 min	49.1±5.50 %.	45±9.11 %.

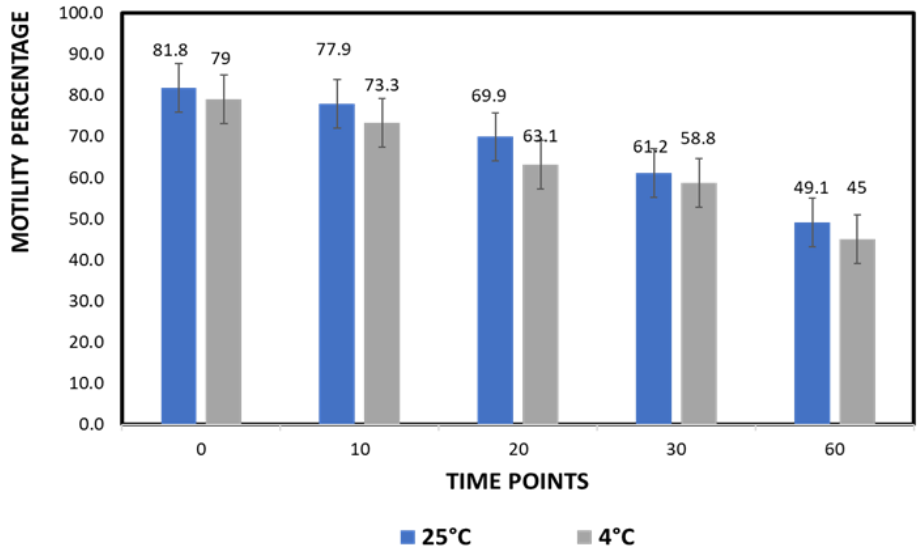

Fig. 3.2 Sperm motility observed under two different incubation temperatures estimated by Phase contrast microscopy.

It can be summarized from table 3.1 that, when the semen samples were processed at 25 °C, the cells were more motile than at 4 °C. The reduction in motility percentage is very feeble as seen in Fig. 3.2. Initially at t= 0 minutes the motility percentage recorded at 25 °C temperature was 81.8±4 % and at 4 °C, the motility percentage was 79±4 %. However, at t= 60 minutes the motility decreased to 49.1±5.50 % at 25 °C. The data was analysed with the help of CASA and is an average of 30 semen straws. To crosscheck the above observation, we stained the same sample with Propidium iodide at t= 0, 10,

20,30, and 60 minutes. The number of cells that fluoresces increases with an increase in the incubation time i.e., the number of dead cells increases with time.

Figure 3.3 shows the fluorescence emission images of PI stained cells at different time points (T= 0, 10, 20, 30, 60 minutes) , it can be seen that, at T=0 minute (Fig. 3.3b) the cells show less amount of fluorescence than at T= 60 minute (Fig. 3.3j).Hence, the number of fluorescent cells increases with time, suggesting that cellular viability is reducing with time. As inferred from the data, the insemination has to be done within 10-15 minutes of thawing the sample, after that the cell viability starts to decrease.

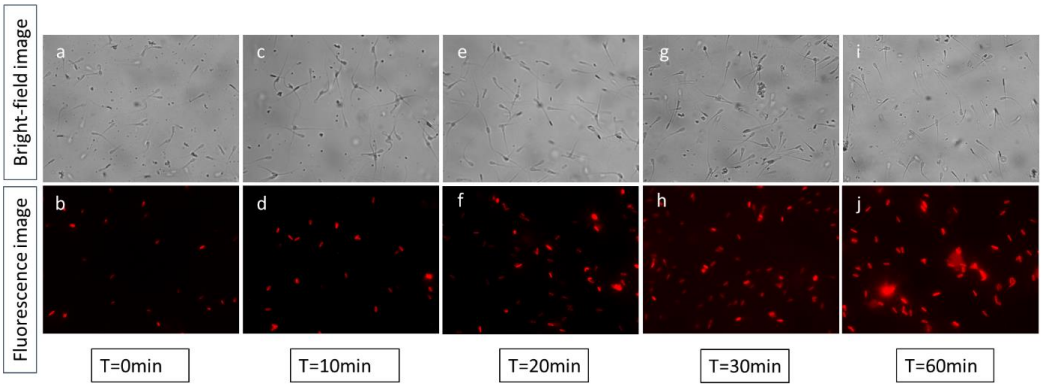

Fig. 3.3: Fluorescence images of dead sperm using Propidium Iodide as observed under fluorescence microscope at different time points.

3.2 Magnetic labelling of sperms using Annexin V conjugated microbeads

The sorting of dead and defective sperm cells is purely based on selective binding of the Annexin V conjugated microbeads to phosphatidylserine (PS) moieties present on the outer leaflet of the lipid bilayer in dead cells, as shown in Fig. 3.4. In live cells the PS moieties are present in the inner leaflet of the lipid bilayer but in dead cells the PS moieties flips outside, and comes to the outer leaflet of the lipid bilayer (Fig. 3.4a and Fig.3.4b). The set up is paired with the neodymium magnet and, the Annexin V conjugated microbeads bind to the PS moieties of the dead sperm cells and the microbeads being magnetic in nature gets attracted to the neodymium magnet, while the live cells get

eluted out as depicted in Fig 3.4c and Fig 3.4d. In order to separate the dead and defective cells we used the magnetic isolation of such cells.

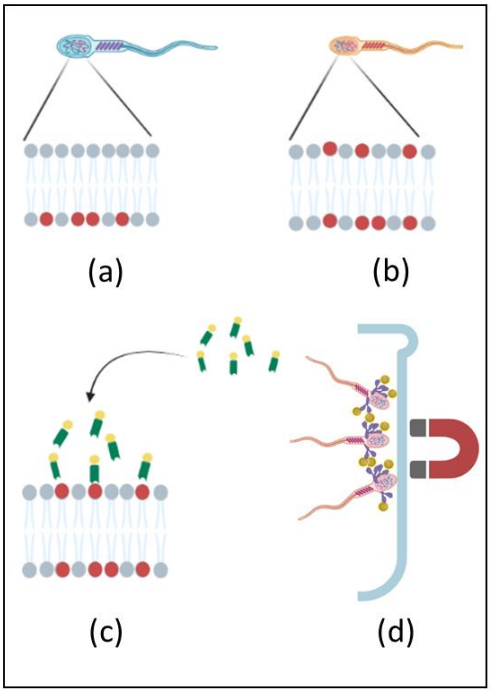

Fig. 3.4: Magnetic separation of non-viable sperm cells from unsorted semen sample (a) section of cell membrane of live sperm showing phosphatidyl serine in the inner leaflet of the bilayer, (b) section of cell membrane of dead sperm where the phosphatidyl serine has flipped outside, (c) Annexin V tagged microbeads attaching to the phosphatidyl serine moieties present on the outer leaflet of bilayer, (d) the magnetic beads conjugated with Annexin V-bound sperm cells getting attracted towards the magnet.

Figure 3.5 shows that most of the magnetic microbead conjugated annexin V bind mostly to the neck and head region of the sperm cells and not to the tail region or any other part of the sperm cells. The primary reason can be that the expression of phosphatidyl serine is more in the head region of the sperm cells. This differential expression of PS moieties in dead cells might lead to binding of Annexin V – microbead to the PS moieties.

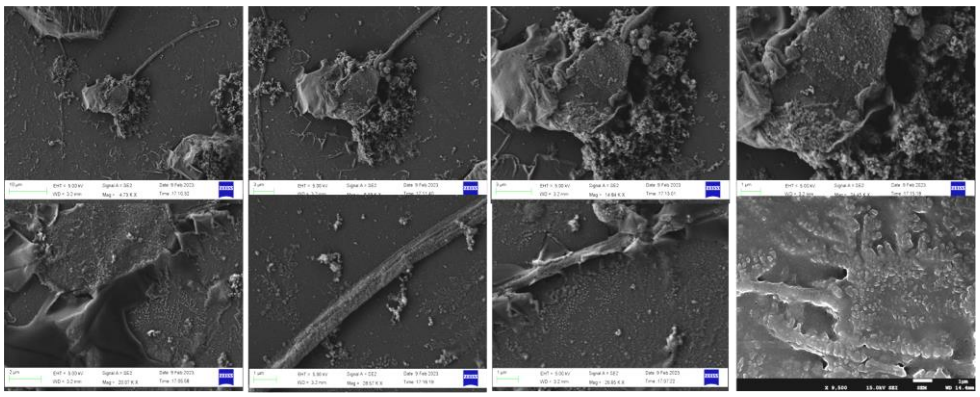

Fig. 3.5: SEM images of Annexin-V conjugated microbead bound sperms.

3.3 Live and dead sperm detection before and after enrichment assay

Before the enrichment assay, there were a lot of dead sperm cells in the sample population however after separation the dead fraction reduced significantly. Figure 3.6 shows fluorescence emission before enrichment due to FITC attached annexin V. after separation there is negligible emission. For this experiment, FITC conjugated Annexin V antibodies were used to stain the cells before and after the experiment. After the sample has been passed through the column, the eluted fraction constitutes mostly of live cells, we have visualized these cells under a fluorescence microscope. The result depicted that before separation, significant FITC fluorescence is detected within the sample population. However, after separation, the fluorescence signal for FITC was not seen in the sperm population. In Figure 3.6, the first column shows bright field images, the second column shows the fluorescence images and the third shows the merged images of the cells. From the observation we can infer that separation strategy was highly useful and efficient. This suggests that magnetically labelled dead cells get immobilized within the Magnet Activated Cell Sorter (MACS) column while the live cells get eluted in flow through [59]. The overall result shows that MACS technology offers a great platform for live and dead separation to achieve a high reproduction rate in the bovine.

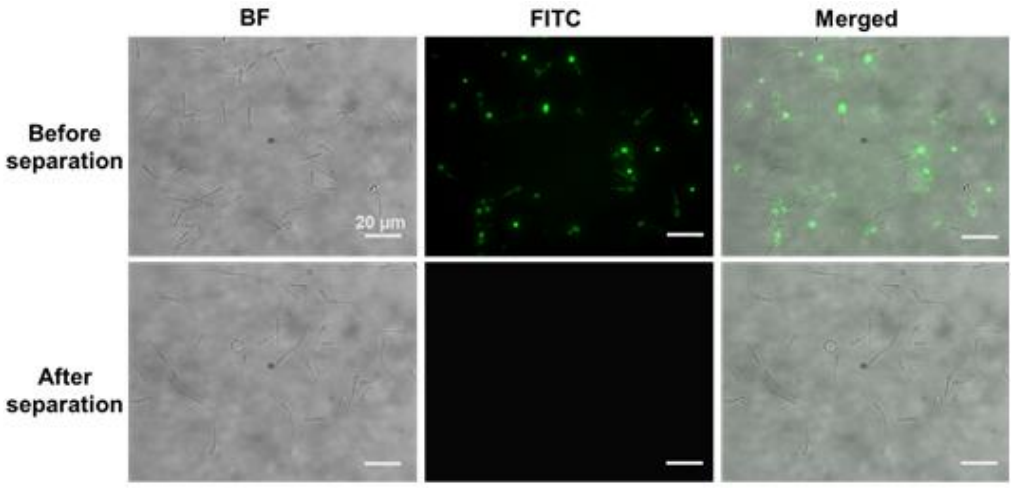

Fig. 3.6: Fluorescence bioimaging of sperms before and after the enrichment assay.

The same experiment was repeated with a different dye, propidium iodide which also stains the dead cells. In the Fig. 3.7a-Fig. 3.7l shows the bright field, fluorescence image and their merged images. It shows that the number of dead cells is much higher before the enrichment assay. However, the number of dead cells decreases drastically after the enrichment assay as seen in Fig. 3.7m-Fig. 3.7x. . In Figure 3.7, the first column shows bright field images, the second column shows the fluorescence images and the third shows the merged images of the cells. Figure 3.8 shows the graphical representation of the number of motile sperms before and after the enrichment assay. Cumulative data of about 120 field of views were taken into consideration and Videos of the motile cells were recorded in the CASA system and the number of motile sperms were counted from there. The percentage of motile cells increased to ~90% post enrichment assay. This suggest that enriched cells might have superior fertility in comparison with un-enriched cells.

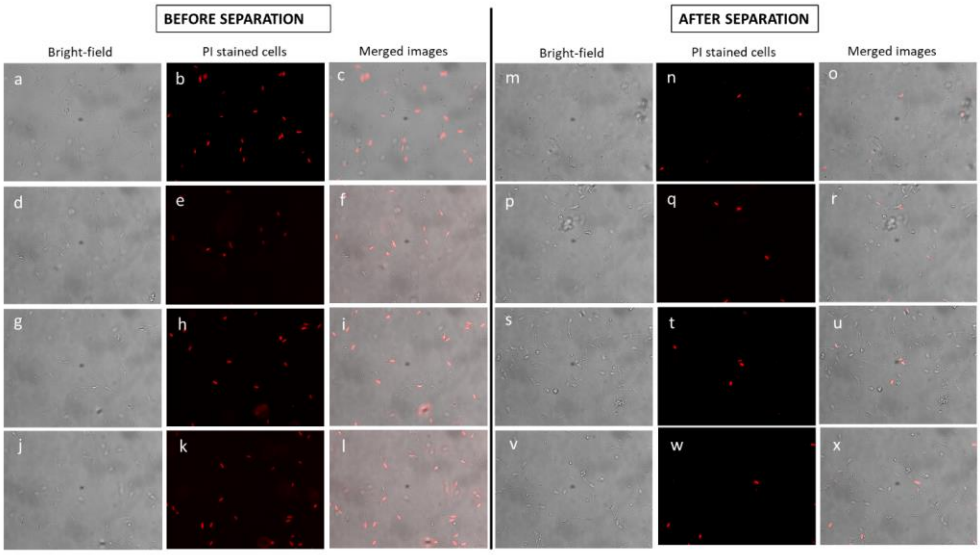

Fig. 3.7: Propidium Iodide staining of sperm cells before and after enrichment assay showing the bright field images, PI-stained cells, and merged images in fluorescence microscope under 40X magnification. Image (a)-(l) shows bright field, propidium iodide stained and merged images of sperm cells before separation. (m)-(x) shows bright field, propidium iodide stained and merged images of sperm cells after separation.

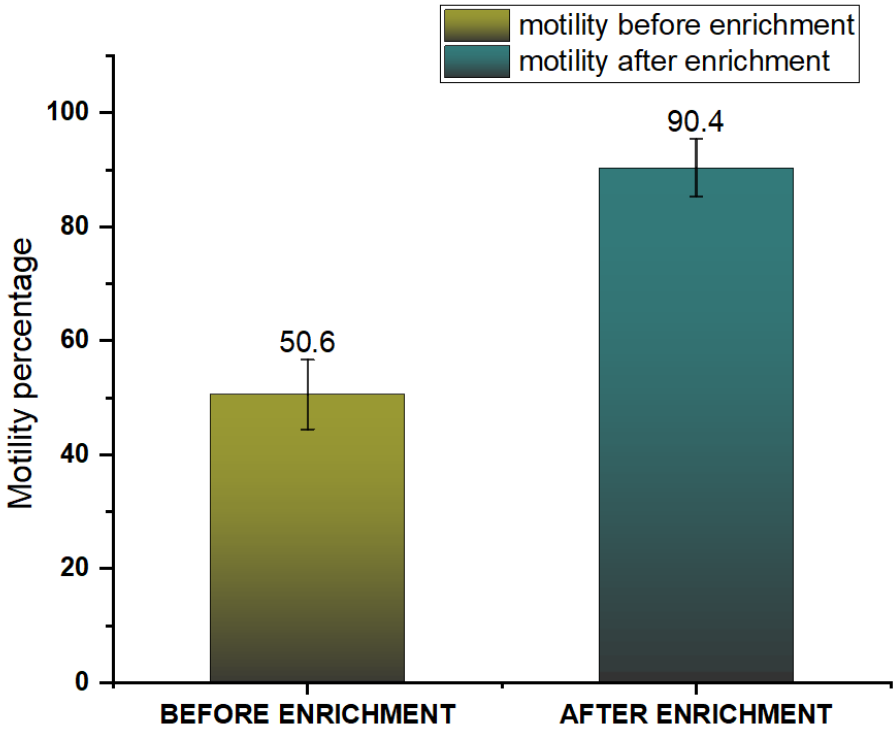

Fig. 3.8: Sperm motility percentage before and after enrichment assay.

3.4 Optical tweezer Raman spectroscopy for sperm identification

Two sets of semen sample were collected from the veterinary doctor and stored in liquid nitrogen at -196°C. Sorted and unsorted semen samples were then preprocessed as described earlier and a 5 µl drop was casted on the slides that were prepared for Raman spectroscopy.

3.4.1 Unsorted semen sample

The raw Raman spectrum of the Unsorted sample as seen below, depicts the cumulative spectra of 50 individual cells. Each cell was trapped in the matrix by optical tweezer and spectrum from the head region was taken. We kept the power constant at 1W and took Raman spectra of 50 different cells. The major peaks are shown in Fig. 3.9 are at 833 cm^{-1}, 970 cm^{-1}, 1319 cm^{-1}, 1420 cm^{-1}, 1637 cm^{-1}. Figure 3.10 shows the standard deviation of all the 50 cells and their mean (red color coded).

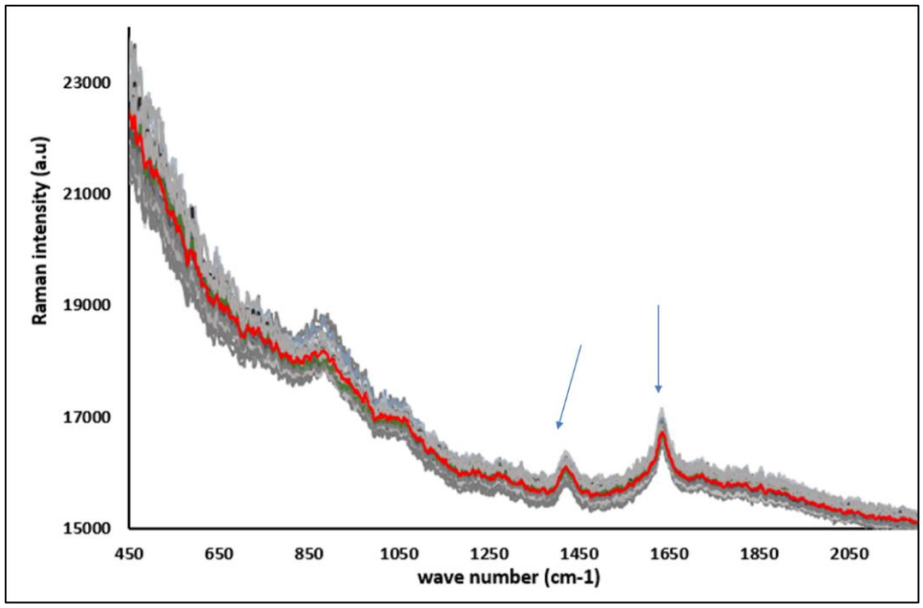

Fig. 3.9: Raw Raman spectral data of unsorted data showing the different peaks and the mean of all the 50 individual data recorded in the setup is denoted by the red line. The grey lines show individual data of the 50 cells.

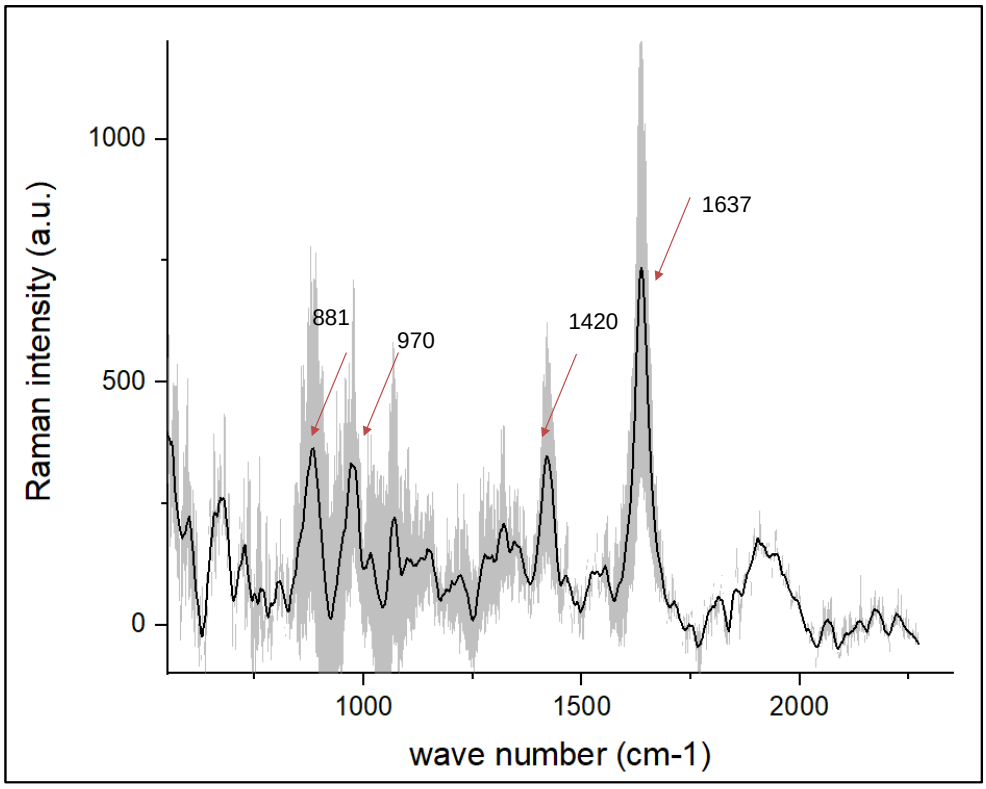

Fig 3.10: Averaged Raman Specra of 50 unsorted sperm cells with the standard deviation after background removal.

3.4.2 Pre-sorted Bovine sperm samples

The Raman spectrum of the Sorted sample as seen in figure 3.11 depicts cumulative of 50 individual cells. Each cell was trapped in the matrix by optical tweezer and spectrum from the head region was taken. All the readings were taken at 1W power and was maintained throughout the experiments. The major peaks we are getting are at 833 cm^{-1}, 970 cm^{-1}, 1104 cm^{-1}, 1319 cm^{-1}, 1420 cm^{-1}, 1637 cm^{-1}. The peaks are majorly similar in between the sorted and unsorted sperm cells however there is a peak difference at 1104 cm^{-1} as seen in Fig. 3.13. Figure 3.12 shows the standard deviation of all the 50 cells and their mean.

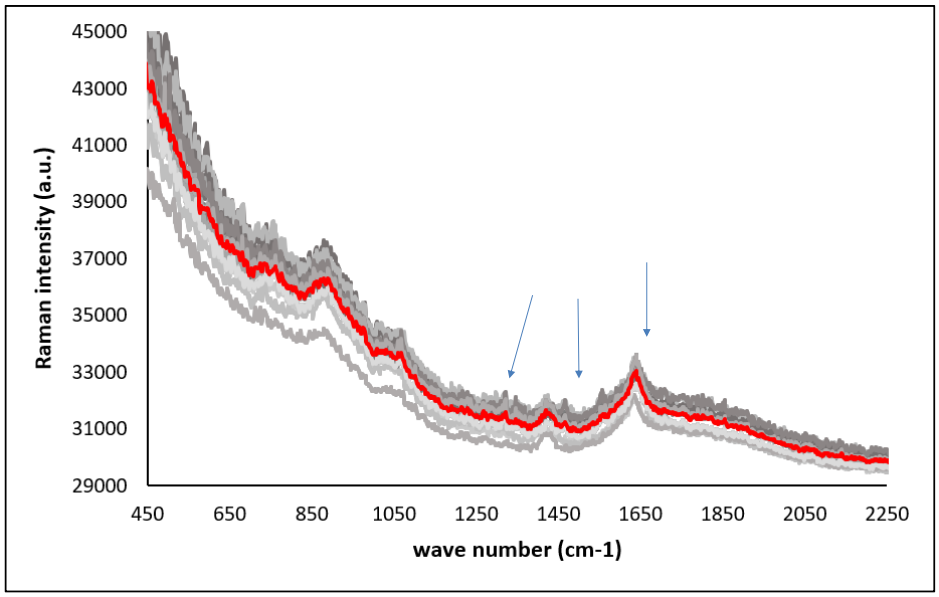

Fig 3.11 : Raw Raman spectral data of the unsorted cells showing the different peaks obtained and the mean of all the 50 individual data recorded in the setup is denoted by the red line. The grey lines show individual data of the 50 cells

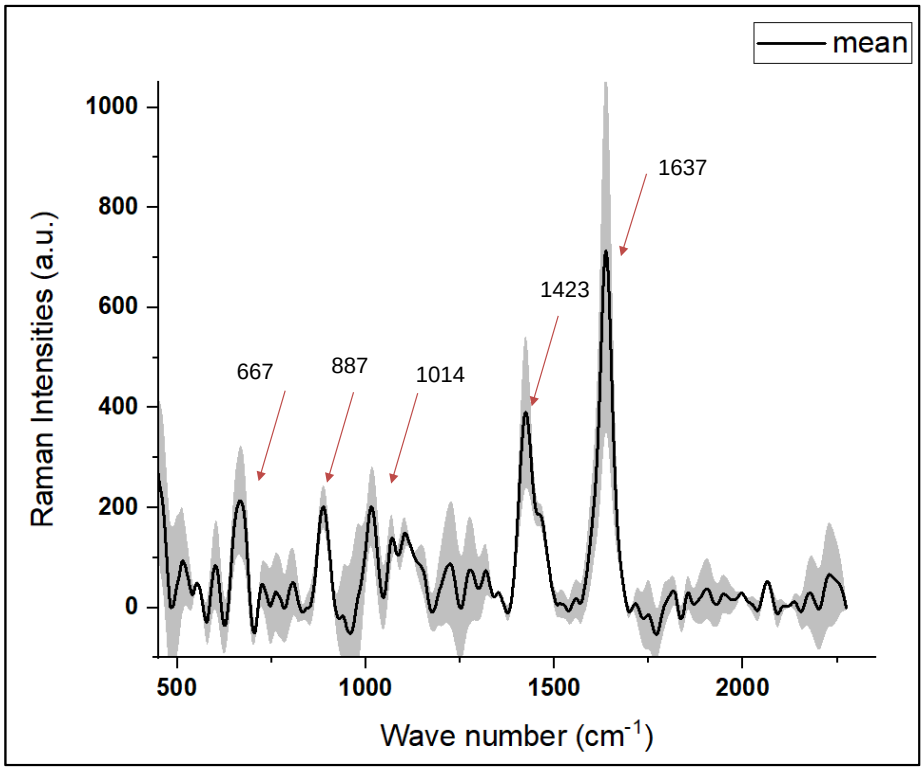

Fig. 3.12: Averaged Raman Specra of 50 sorted sperm cells with the standard deviation after background removal.

The merged data shown in Fig. 3.13 shows the different peaks obtained in the sorted and the unsorted data sets. The range from 1200 cm^{-1} to 1400 cm^{-1} shows the signature peaks of DNA, Adenine and Guanine. However, the peak at 1650 also depicts a signature peak of DNA, the major peak difference we are getting are at 970 cm^{-1},1014 cm^{-1}, 1070 cm^{-1} , and 1319 cm^{-1}. The sorted sample shows a higher intensity than the unsorted and the main reason of this difference is due to the presence of 4 % more DNA in the sorted sample than the unsorted sample. Table 3.2 shows the reference from which we analysed the peaks of different components and the molecular origins of those peaks.

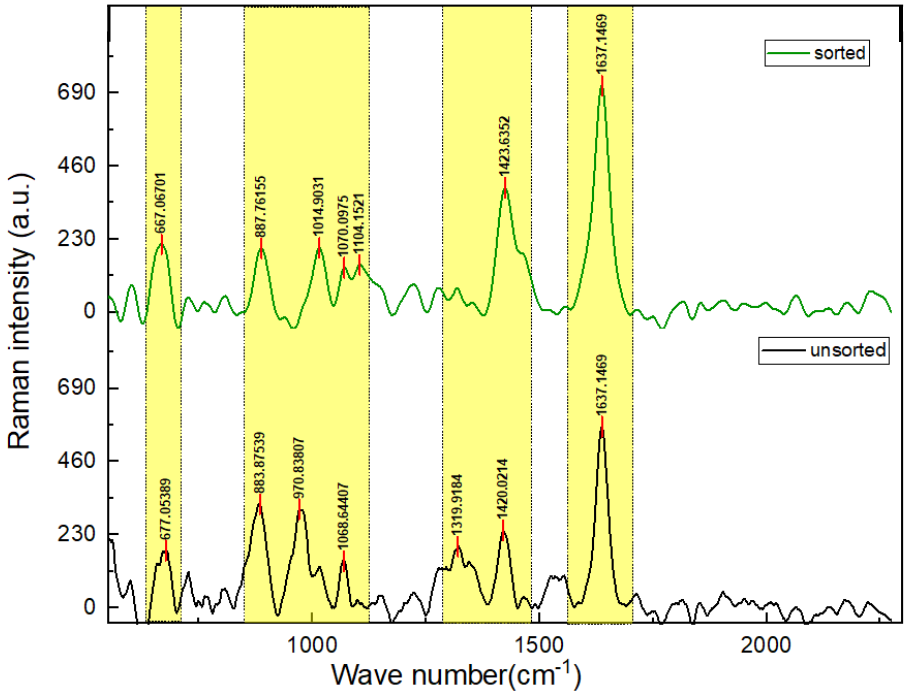

Fig. 3.13: Stacked up graph plots of sorted and unsorted Raman spectrum.

Table 3.2: Wavelength of the respective peaks observed in Raman spectroscopy [60-62].

Wavenumber(cm^{-1})	**Vibrational mode**	**Molecular origin**
667	Ring deformation	Seminal fluid
883	Phosphodiester, Deoxyribose	DNA, thymine, cytosine, uracil
920-970	C-C stretching	Ribose Phosphate
1104	PO^{2-}	DNA backbone
1227	C-C	DNA
1319	CH3CH2 twisting	Adenine
1343		Adenine, guanine
1420	Amide I	Protein
1637		Adenine, thymine

Chapter 4

Conclusion and Future Prospect

The proposed protocol for live and dead sperm sorting using fluorophore-magnetic microbead conjugate in a magnetic environment successfully removed the majority of the dead and defective sperms. This a simple methodology for dead sperm sorting that can serve the purpose well and help the conception rate. Flow cytometry-based cell sorting exposes sperms to high pressures that result in DNA damage. The methodology discussed in this thesis requires a simple setup and the sperms are not subjected to high pressure or temperature. Our method is non-invasive and cost effective. In addition to removal of dead and defective sperms. In addition to this we used OTRS for sperm identification where we could see a clear difference in intensities between the sorted and the unsorted cells. This difference in intensity can be directly related to the difference in DNA content between the sorted which contains more population of X-sperms and the unsorted cells which contain equal population of X and Y cells. The X-spermatozoa containing more DNA content has a higher intensity peak than the Y-spermatozoa.

Raman spectroscopy is a non-invasive and non-destructive technique that does not require sample labelling or fixation, making it an attractive alternative to traditional methods of semen sexing, such as flow cytometry, it can be analyzed to determine the ratio of X and Y chromosome-bearing sperm cells. Raman spectroscopy can also be used to analyse the chemical composition of other components of the semen sample, such as proteins, lipids, and nucleic acids. These components can provide additional information about the quality and fertility of the semen sample. In the future OTRS can provide a staining free approach for semen sexing.

References

[1] A. Khanna, S. Jain, A. Burgio, V. Bolshev, and V. Panchenko, 'Blockchain-Enabled Supply Chain platform for Indian Dairy Industry: Safety and Traceability', Foods 2022, Vol. 11, Page 2716, vol. 11, no. 17, p. 2716, Sep. 2022, https://doi.org/10.3390/FOODS11172716

[2] P. Rupala, 'India ranks first in milk production in the world contributing 24% of global milk production', Delhi, Feb. 2023. Accessed: May 01, 2023. [Online]. Available: https://pib.gov.in/PressReleaseIframePage.aspx?PRID=1897084

[3] P. Mishra, A. Matuka, M. S. A. Abotaleb, W. P. M. C. N. Weerasinghe, K. Karakaya, and S. S. Das, 'Modeling and forecasting of milk production in the SAARC countries and China', Model Earth Syst Environ, vol. 8, no. 1, pp. 947–959, Mar. 2022, https://doi.org/10.1007/S40808-021-01138-Z/TABLES/12

[4] D. Zuidema, K. Kerns, and P. Sutovsky, 'An Exploration of Current and Perspective Semen Analysis and Sperm Selection for Livestock Artificial Insemination', Animals 2021, Vol. 11, Page 3563, vol. 11, no. 12, p. 3563, Dec. 2021, https://doi.org/10.3390/ANI11123563

[5] S. G. Moore and J. F. Hasler, 'A 100-Year Review: Reproductive technologies in dairy science', J Dairy Sci, vol. 100, no. 12, pp. 10314–10331, Dec. 2017, https://doi.org/10.3168/JDS.2017-13138

[6] D. R. Lyngkhoi, S. B. Singh, R. Singh, and H. Tyngkan, 'Trend Analysis of Milk Production in India', Asian Journal of Dairy and Food Research, vol. 41, no. 2, pp. 183–187, Jun. 2022, https://doi.org/10.18805/AJDFR.DR-1789

[7] W. A. Khalil, M. A. El-Harairy, A. E. B. Zeidan, M. A. E. Hassan, and O. Mohey-Elsaeed, 'Evaluation of bull spermatozoa during and after cryopreservation: Structural and ultrastructural insights', Int J Vet Sci Med, vol. 6, pp. S49–S56, Jan. 2018, https://doi.org/10.1016/J.IJVSM.2017.11.001

[8] M. R. Ugur et al., 'Advances in Cryopreservation of Bull Sperm', Front Vet Sci, vol. 6, Aug. 2019, https://doi.org/10.3389/FVETS.2019.00268

[9] A. Kumar, J. Prasad, … N. S.-B. and, and undefined 2019, ‘Strategies to minimize various stress-related freeze–thaw damages during conventional cryopreservation of mammalian spermatozoa’, liebertpub.com, vol. 17, no. 6, pp. 603–612, Dec. 2019, https://doi.org/10.1089/bio.2019.0037

[10] N. H.-A. at S. 4345390 and undefined 2019, ‘Livestock development for sustainable livelihood of small farmers’, papers.ssrn.com, vol. 3, no. 2, pp. 1–17, 2019, Accessed: May 01, 2023. [Online]. Available: https://papers.ssrn.com/sol3/papers.cfm?abstract_id=4345390

[11] I. Yánez-Ortiz, J. Catalán, J. E. Rodríguez-Gil, J. Miró, and M. Yeste, ‘Advances in sperm cryopreservation in farm animals: Cattle, horse, pig and sheep’, Anim Reprod Sci, vol. 246, Nov. 2022, https://doi.org/10.1016/J.ANIREPROSCI.2021.106904

[12] D. L. Garner and G. E. Seidel, ‘Past, present and future perspectives on sexing sperm’, Can J Anim Sci, vol. 83, no. 3, pp. 375–384, 2003, https://doi.org/10.4141/A03-022

[13] T. J. Manuel, M. Maria Jose, C. Adriana Maria, Z. Carlos, and M. P. Estela, ‘Use of Annexin V based Sperm Selection in Assisted Reproduction’, J Antimicrob Agents, vol. 06, no. 01, 2017, https://doi.org/10.4172/2167-0250.1000182

[14] D. Garner, K. Evans, G. S.-S. M. and, and undefined 2013, ‘Sex-sorting sperm using flow cytometry/cell sorting’, Springer, pp. 279–295, 2013, https://doi.org/10.1007/978-1-62703-038-0_26

[15] J. Gosálvez et al., ‘Sex-sorted bovine spermatozoa and DNA damage: I. Static features’, Theriogenology, vol. 75, no. 2, pp. 197–205, Jan. 2011, https://doi.org/10.1016/J.THERIOGENOLOGY.2010.08.006

[16] T. K. Suh, J. L. Schenk, and G. E. Seidel, ‘High pressure flow cytometric sorting damages sperm’, Theriogenology, vol. 64, no. 5, pp. 1035–1048, Sep. 2005, https://doi.org/10.1016/J.THERIOGENOLOGY.2005.02.002

[17] H. Pathak, ‘Transforming the Agri-food Sector in India for Achieving the Sustainable Development Goals’, Anthropocene Science 2023 2:1, vol. 2, no. 1, pp. 1–4, Feb. 2023, https://doi.org/10.1007/S44177-023-00044-6

[18] M. Thongkham, W. Thaworn, W. Pattanawong, S. Teepatimakorn, S. Mekchay, and K. Sringarm, ‘Spermatological parameters of immunologically sexed bull semen assessed by imaging flow cytometry, and dairy farm trial’, Reprod Biol, vol. 21, no. 2, p. 100486, Jun. 2021, https://doi.org/10.1016/J.REPBIO.2021.100486

[19] S. G. Jr and G. DL, ‘Current status of sexing mammalian spermatozoa.’, Reproduction, vol. 124, no. 6, pp. 733–743, Dec. 2002, https://doi.org/10.1530/REP.0.1240733

[20] M. Gil, V. Sar-Shalom, Y. Melendez Sivira, R. Carreras, and M. A. Checa, ‘Sperm selection using magnetic activated cell sorting (MACS) in assisted reproduction: a systematic review and meta-analysis.’, J Assist Reprod Genet, vol. 30, no. 4, pp. 479–485, 2013, https://doi.org/10.1007/S10815-013-9962-8

[21] T. S. Berteli, M. G. Da Broi, W. P. Martins, R. A. Ferriani, and P. A. Navarro, ‘Magnetic-activated cell sorting before density gradient centrifugation improves recovery of high-quality spermatozoa’, Andrology, vol. 5, no. 4, pp. 776–782, Jul. 2017, https://doi.org/10.1111/ANDR.12372

[22] C. de Vantéry Arrighi, H. Lucas, D. Chardonnens, and A. de Agostini, ‘Removal of spermatozoa with externalized phosphatidylserine from sperm preparation in human assisted medical procreation: effects on viability, motility and mitochondrial membrane potential.’, Reprod Biol Endocrinol, vol. 7, p. 1, 2009, https://doi.org/10.1186/1477-7827-7-1

[23] Z. Beyhan, L. A. Johnson, and N. L. First, ‘Sexual dimorphism in IVM-IVF bovine embryos produced from x and y chromosome-bearing spermatozoa sorted by high-speed flow cytometry’, Theriogenology, vol. 52, no. 1, pp. 35–48, Jul. 1999, https://doi.org/10.1016/S0093-691X(99)00108-9

[24] O. Olatunji and A. More, ‘A Review of the Impact of Microfluidics Technology on Sperm Selection Technique’, Cureus, Jul. 2022, https://doi.org/10.7759/CUREUS.27369

[25] S. L. Underwood, C. Vigneault, and P. Blondin, ‘Flow Cytometric Sorting of Mammalian Sperm for Predetermination of Sex’, in

Comprehensive Biotechnology, Second Edition, Elsevier Inc., 2011, pp. 430–440. https://doi.org/10.1016/B978-0-08-088504-9.00285-3

[26] L. Z. Oliveira et al., 'Transmission electron microscopy for characterization of acrosomal damage after Percoll gradient centrifugation of cryopreserved bovine spermatozoa', J Vet Sci, vol. 12, no. 3, pp. 267–272, 2011, https://doi.org/10.4142/JVS.2011.12.3.267

[27] A. Chaveiro, P. Santos, and F. M. Da Silva, 'Assessment of sperm apoptosis in cryopreserved bull semen after swim-up treatment: A flow cytometric study', Reproduction in Domestic Animals, vol. 42, no. 1, pp. 17–21, Feb. 2007, https://doi.org/10.1111/J.1439-0531.2006.00712.X

[28] J. J. PARRISH and R. H. FOOTE, 'Quantification of Bovine Sperm Separation by a Swim-up Method Relationship to Sperm Motility, Integrity of Acrosomes, Sperm Migration in Polyacrylamide Gel and Fertility', J Androl, vol. 8, no. 4, 1987, https://doi.org/10.1002/j.1939-4640.1987.tb03319.x

[29] M. Gil, V. Sar-Shalom, Y. Melendez Sivira, R. Carreras, and M. A. Checa, 'Sperm selection using magnetic activated cell sorting (MACS) in assisted reproduction: a systematic review and meta-analysis.', J Assist Reprod Genet, vol. 30, no. 4, pp. 479–485, 2013, https://doi.org/10.1007/S10815-013-9962-8

[30] A. Janshoff, M. Ross, V. Gerke, and C. Steinem, 'Visualization of annexin I binding to calcium-induced phosphatidylserine domains', ChemBioChem, vol. 2, no. 7–8, 2001, https://doi.org/10.1002/1439-7633(20010803)2:7/8<587::aid-cbic587>3.0.co;2-q

[31] J. Sopkova, M. Renouard, and A. Lewit-Bentley, 'The crystal structure of a new high-calcium form of annexin V', J Mol Biol, vol. 234, no. 3, pp. 816–825, Dec. 1993, https://doi.org/10.1006/JMBI.1993.1627

[32] A. Janshoff, M. Ross, V. Gerke, C. S.- ChemBioChem, and undefined 2001, 'Visualization of Annexin I Binding to Calcium-Induced Phosphatidylserine Domains', Wiley Online Library, no. 7, 2001, https://doi.org/10.1002/1439-7633(20010803)2:7/8<587::AID-CBIC587>3.0.CO;2-Q

[33] N. M. Gulaya, V. M. Margitich, N. M. Govseeva, V. M. Klimashevsky, I. I. Gorpynchenko, and M. I. Boyko, 'Phospholipid composition of human sperm and seminal plasma in relation to sperm fertility', Arch Androl, vol. 46, no. 3, pp. 169–175, 2001, https://doi.org/10.1080/01485010151096405

[34] 'Propidium iodide = 94.0 HPLC 25535-16-4'. https://www.sigmaaldrich.com/IN/en/product/sigma/p4170 (accessed May 01, 2023).

[35] N. P. Bazhulina et al., 'Binding of Hoechst 33258 and its Derivatives to DNA', http://dx.doi.org/10.1080/07391102.2009.10507283, vol. 26, no. 6, pp. 701–718, 2012, https://doi.org/10.1080/07391102.2009.10507283

[36] J. Kapuscinski, 'DAPI: A DMA-Specific fluorescent probe', Biotechnic and Histochemistry, vol. 70, no. 5, pp. 220–233, 1995, https://doi.org/10.3109/10520299509108199

[37] P. E. Pjura, K. Grzeskowiak, and R. E. Dickerson, 'Binding of Hoechst 33258 to the Minor Groove of B-DNA', 1987.

[38] P. Jia et al., 'The RGD-modified self-assembling D-form peptide hydrogel enhances the therapeutic effects of mesenchymal stem cells (MSC) for hindlimb ischemia by promoting angiogenesis', Chemical Engineering Journal, vol. 450, Dec. 2022, https://doi.org/10.1016/J.CEJ.2022.138004

[39] J. Bucevičius, G. Lukinavičius, and R. Gerasimaite, 'The use of hoechst dyes for DNA staining and beyond', Chemosensors, vol. 6, no. 2. MDPI Multidisciplinary Digital Publishing Institute, Jun. 01, 2018. https://doi.org/10.3390/chemosensors6020018

[40] 'Magnetic Nanoparticles - Google Books'. https://books.google.co.in/books?hl=en&lr=&id=Cprq0nQC4LYC&oi=fnd&pg=PR5&dq=magnetic+nanoparticles&ots=AvD9ALHayG&sig=i1RSRvJvghRWSx_rzJLaKJROJO0&redir_esc=y#v=onepage&q=magnetic%20nanoparticles&f=false (accessed May 01, 2023).

[41] I. T. K and L. P. K, 'Magnetic Nanoparticles – A Review', International Journal of Pharmaceutical Sciences and Nanotechnology

(IJPSN), vol. 3, no. 3, pp. 1035–1042, Nov. 2010, https://doi.org/10.37285/IJPSN.2010.3.3.1

[42] Z. Gao et al., ‘Preparation of Scalable Silica-Coated Iron Oxide Nanoparticles for Nanowarming’, Advanced Science, vol. 7, no. 4, p. 1901624, Feb. 2020, https://doi.org/10.1002/ADVS.201901624

[43] B. Herman, ‘Fluorescence Microscopy’, Curr Protoc Cell Biol, vol. 00, no. 1, pp. 4.2.1-4.2.10, Oct. 1998, https://doi.org/10.1002/0471143030.CB0402S13

[44] J. W. Lichtman and J. A. Conchello, ‘Fluorescence microscopy’, Nature Methods 2005 2:12, vol. 2, no. 12, pp. 910–919, Nov. 2005, https://doi.org/10.1038/nmeth817

[45] ‘Inverted Fluorescent Microscope (nikon Eclipse Ti-U) | IISER Tirupati’. http://www.iisertirupati.ac.in/inverted-fluorescent-microscope-nikon-eclipse-ti-u/ (accessed May 01, 2023).

[46] ‘Introduction to Fluorescence Microscopy | Nikon’s MicroscopyU’. https://www.microscopyu.com/techniques/fluorescence/introduction-to-fluorescence-microscopy (accessed May 01, 2023).

[47] Q. S. Hanley, ‘Fluorescence Spectroscopy, Imaging and Probes: New Tools in Chemical Physical, and Life Sciences’, J Microsc, vol. 212, no. 2, pp. 212–213, Nov. 2003, https://doi.org/10.1046/J.1365-2818.2003.01255.X

[48] S. Weiss, ‘Fluorescence spectroscopy of single biomolecules’, Science (1979), vol. 283, no. 5408, pp. 1676–1683, Mar. 1999, https://doi.org/10.1126/SCIENCE.283.5408.1676

[49] ‘Instrumentation for Fluorescence Spectroscopy’, Principles of Fluorescence Spectroscopy, pp. 27–61, 2006, https://doi.org/10.1007/978-0-387-46312-4_2

[50] R. L. Burns et al., ‘A Fast, Straightforward and Inexpensive Method for the Authentication of Baijiu Spirit Samples by Fluorescence Spectroscopy’, Beverages 2021, Vol. 7, Page 65, vol. 7, no. 3, p. 65, Sep. 2021, https://doi.org/10.3390/BEVERAGES7030065

[51] C. A. Royer, ‘Fluorescence spectroscopy.’, Methods Mol Biol, vol. 40, pp. 65–89, 1995, https://doi.org/10.1385/0-89603-301-5:65/COVER

[52] M. Li et al., ‘Evaluation of Laser Confocal Raman Spectroscopy as a Non-Invasive Method for Detecting Sperm DNA Contents’, Front Physiol, vol. 13, p. 102, Feb. 2022, https://doi.org/10.3389/FPHYS.2022.827941/BIBTEX

[53] A. Kumar, ‘General rights Understanding defect related luminescence processes in wide bandgap materials using low temperature multi-spectroscopic techniques’, 2017.

[54] A. De Angelis et al., ‘Spermatozoa quality assessment: a combined holographic and Raman microscopy approach’, in Optical Methods for Inspection, Characterization, and Imaging of Biomaterials II, SPIE, Jun. 2015, p. 952916. https://doi.org/10.1117/12.2186393

[55] S. Du et al., ‘Micro-Raman Analysis of Sperm Cells on Glass Slide: Potential Label-Free Assessment of Sperm DNA toward Clinical Applications’, Biosensors 2022, Vol. 12, Page 1051, vol. 12, no. 11, p. 1051, Nov. 2022, https://doi.org/10.3390/BIOS12111051

[56] M. A. Ferrara et al., ‘Label-free imaging and biochemical characterization of bovine sperm cells’, Biosensors (Basel), vol. 5, no. 2, pp. 141–157, 2015, https://doi.org/10.3390/bios5020141

[57] M. A. Fikiet and I. K. Lednev, ‘Raman spectroscopic method for semen identification: Azoospermia’, Talanta, vol. 194, pp. 385–389, Mar. 2019, https://doi.org/10.1016/J.TALANTA.2018.10.034

[58] Y. Singh, A. Chowdhury, C. Mukherjee, R. Dasgupta, and S. K. Majumder, ‘Simultaneous photoreduction and Raman spectroscopy of red blood cells to investigate the effects of organophosphate exposure’, J Biophotonics, 2019, https://doi.org/10.1002/jbio.201800246

[59] T. I. de Assumpção, N. C. Severo, J. P. B. Zandonaide, and G. G. Macedo, ‘Magnetic-activated cell sorting improves high-quality spermatozoa in bovine semen’, Journal of Animal Reproduction and Biotechnology, vol. 36, no. 2, pp. 91–98, Jun. 2021, https://doi.org/10.12750/JARB.36.2.91

[60] Y. Singh, A. Chowdhury, C. Mukherjee, R. Dasgupta, and S. K. Majumder, ‘Simultaneous photoreduction and Raman spectroscopy of red blood cells to investigate the effects of organophosphate exposure’, J

Biophotonics, vol. 12, no. 5, p. e201800246, May 2019, https://doi.org/10.1002/JBIO.201800246

[61] A. de angelis et al., ‘Spermatozoa quality assessment: A combined holographic and Raman microscopy approach’, Proceedings of SPIE - The International Society for Optical Engineering, vol. 9529, Apr. 2015, https://doi.org/10.1117/12.2186393

[62] M. A. Fikiet and I. K. Lednev, ‘Raman spectroscopic method for semen identification: Azoospermia’, Talanta, vol. 194, pp. 385–389, Mar. 2019, https://doi.org/10.1016/J.TALANTA.2018.10.034

[63] S. Du et al., ‘Micro-Raman Analysis of Sperm Cells on Glass Slide: Potential Label-Free Assessment of Sperm DNA toward Clinical Applications’, Biosensors 2022, Vol. 12, Page 1051, vol. 12, no. 11, p. 1051, Nov. 2022, https://doi.org/10.3390/BIOS12111051